



## Research article

# First report of the complete mitochondrial genome of *Carpomya pardalina* (Bigot) (Diptera: Tephritidae) and phylogenetic relationships with other Tephritidae

Xianting Guo<sup>a</sup>, Hualing Wang<sup>b</sup>, Kaiyun Fu<sup>c</sup>, Xinhua Ding<sup>c</sup>, Jianyu Deng<sup>a,\*\*</sup>,  
Wenchao Guo<sup>c,\*\*\*</sup>, Qiong Rao<sup>a,\*</sup>

<sup>a</sup> Key Lab for Biology of Crop Pathogens and Insect Pests and Their Ecological Regulation of Zhejiang Province, College of Advanced Agricultural Sciences, Zhejiang A & F University, Hangzhou, 311300, China

<sup>b</sup> College of Forestry, Hebei Agricultural University, Baoding, 071000, Hebei, China

<sup>c</sup> Key Laboratory of Integrated Pest Management on Crops in Northwestern Oasis, Ministry of Agriculture and Rural Affairs, Xinjiang Key Laboratory of Agricultural Bio-safety, Institute of Plant Protection, Xinjiang Academy of Agricultural Sciences, Urumqi, Xinjiang, 830091, China

## ARTICLE INFO

## Keywords:

Mitochondrial genome  
Phylogenetic analysis  
Tephritidae  
*Carpomya pardalina*

## ABSTRACT

*Carpomya pardalina* is known for its potential invasiveness, which poses a significant and alarming threat to Cucurbitaceae crops. It is considered a highly perilous pest species that requires immediate attention for quarantine and prevention. Due to the challenges in distinguishing pests of the Tephritidae family based on morphological characteristics, it is imperative to elucidate the mitochondrial genomic information of *C. pardalina*. In this study, the mitochondrial genome sequence of *C. pardalina* was determined and analyzed using next-generation sequencing. The results revealed that the mitogenome sequence had a total length of 16,257 bp, representing a typical circular molecule. It consisted of 13 PCGs, two rRNA genes, 22 tRNA genes and a non-coding region. The structure and organization of the mitochondrial genome of *C. pardalina* were found to be typical and similar to the published homologous sequences of other fruit flies in the Tephritidae family. Phylogenetic analysis confirmed that *C. pardalina* belongs to the *Carpomya* genus, which is consistent with traditional morphological taxonomy. Additionally, *Carpomya* and *Rhagoletis* were identified as sister groups. This study presents the first report of the complete mitochondrial genome of *C. pardalina*, which can serve as a valuable resource for future investigations in species diagnosis, evolutionary biology, prevention and control measures.

## 1. Introduction

*Carpomya pardalina* (Bigot) (Diptera: Tephritidae), commonly referred to as *Myiopardalis pardalina*, primarily inflicts damage on plants of Cucurbitaceae family, including melon, watermelon, and cucumber [1,2]. The adult flies deposit their eggs beneath the skin of fresh melons. Upon hatching, the larvae penetrate the fruit and feed on the flesh, causing substantial decay and rotting of the affected melons. The tissue of the melon that is destroyed by the larvae undergoes browning, resulting in the loss of flavor and aroma.

\* Corresponding author.

\*\* Corresponding author.

\*\*\* Corresponding author.

E-mail addresses: [jydeng70@aliyun.com](mailto:jydeng70@aliyun.com) (J. Deng), [gwc1966@163.com](mailto:gwc1966@163.com) (W. Guo), [qiong.rao@zafu.edu.cn](mailto:qiong.rao@zafu.edu.cn) (Q. Rao).

<https://doi.org/10.1016/j.heliyon.2024.e29233>

Received 11 September 2023; Received in revised form 31 March 2024; Accepted 3 April 2024

Available online 11 April 2024

2405-8440/© 2024 The Authors. Published by Elsevier Ltd. This is an open access article under the CC BY-NC license (<http://creativecommons.org/licenses/by-nc/4.0/>).

As the larvae reach maturity, they burrow out of the melon's outer skin of the melon and proceed to pupate in the soil. Furthermore, the damaged fruits are highly susceptible to bacterial and fungal infections [3]. The original range of the *C. pardalina* was the Middle East, the Caucasus and West Asia, where it has been present for at least 100 years. Subsequently, it started to invade Central Asian countries such as Kazakhstan, Afghanistan, Turkmenistan, Uzbekistan, and Tajikistan [3]. In 1980, the invasion of *C. pardalina* was detected in Afghanistan, and in 2004, it was also detected in Kazakhstan [4]. Since 2011, the yield of *Cucumis melo* has suffered damage ranging from 10% to 25%, and even complete loss in some areas [5]. *C. pardalina* is a serious pest that spreads quickly, and its host plants are widely distributed in China. Xinjiang, an important commercial hub in Eurasia, engages in frequent trade of agricultural products both domestically and internationally. There is a high risk of *C. pardalina* being introduced into the highly fertile areas of China's interior through the transportation of agricultural products. Once introduced, this pest will have a devastating impact on the relevant industries [3–5]. Traditionally, the identification of Tephritidae pests has relied mainly on morphological methods [6,7]. However, during the quarantine of fruits and vegetables, larvae and eggs of Tephritidae pests are frequently intercepted. It is challenging to identify the larvae and pupae of Tephritidae pests to the species level based solely on morphology. In contrast, the identification of *C. pardalina* can be rapidly identified using molecular marker technology. However, only a partial sequence of the *COX1* gene of *C. pardalina* is available in the GeneBank database, while the complete mitochondrial genome sequences of *C. incompleta* and *C. vesuviana* have been reported [8]. Furthermore, there is a lack of studies on the relationship between *C. pardalina* and other species within the Tephritidae family.

Insect mitochondrial genomes are the most extensively studied group in the Arthropoda, comprising 80% of the total [9]. Mitochondrial genomes have been obtained for every major suborder, with a focus on Lepidoptera, Hemiptera, Hymenoptera, Coleoptera, Orthoptera, and Diptera [10–15]. The mitochondrial genome is a valuable resource with easily amplified sequences, a stable gene number, a rapid evolutionary rate, a low recombination frequency, and strict matrilineal inheritance [16–18]. These characteristics have contributed to its extensive use in phylogenetic analyses at both the intraspecific and interspecific levels [18]. The insect mitochondrial genome typically exhibits a closed circular double-stranded molecular structure, which comprises two genes encoding ribosomal RNAs (rRNAs), 22 genes encoding transfer RNAs (tRNAs), 13 protein-coding genes (PCGs) and a non-coding region (also called the control region) arranged in a compact sequence [19,20].

In this study, the mitochondrial genome of *C. pardalina* was sequenced and analyzed using high-throughput sequencing technology. Additionally, the study explored the taxonomic position of *C. pardalina* within the Tephritidae family and its genetic relationship with other species in the same family. The results of this study have significant implications for future research on molecular characterization, population genetics research of *C. pardalina*, and phylogenetic studies of the Tephritidae family. The findings also provide offer valuable sequencing information that can contribute to the development of efficient methods for quick detection and quarantine of this pest. Thus, a comprehensive understanding of the genetic characteristics and evolution of *C. pardalina* is crucial for mitigating potential risks, and offers important insights for designing effective control and prevention measures.

## 2. Materials and methods

### 2.1. DNA extraction

The insect sample were collected in July 2021 at Chabuhaer, Xinjiang, China (43.76936737°N, 81.03400926°E). Shortly thereafter, the pest was completely eradicated. The larvae and pupae of *C. pardalina* were immersed in anhydrous alcohol and stored at a temperature of  $-20^{\circ}\text{C}$ . The DNA of *C. pardalina* was extracted using the Rapid Animal Genomic DNA Isolation Kit (Shanghai Sangon Biotech, China) according to the instructions. Then, PCR amplification was performed using universal primers for *COI*, and the resulting PCR products were sent to Shanghai Sangon Biotech for sequencing and subsequent comparison in the NCBI database. The results indicate a 100% sequence similarity between the *COI* gene segment of the samples in this study and the sequences of *C. pardalina* in the database. The extracted DNA was then assessed for integrity using a 1% agarose gel (voltage: 200 V, time: 30 min), and the concentration of the DNA samples was quantified using the Qubit™ dsDNA HS Assay Kit (ThermoFisher, USA).

### 2.2. Mitochondrial genome sequencing and assembly

The DNA of *C. pardalina* larvae were sent to Shanghai Biotechnology Company in China for library construction using the Whole Genome Shotgun (WGS) strategy. A library was prepared with an insert fragment length of approximately 500 bp. DNA fragmentation was conducted using a Covaris ultrasonic DNA fragmentation instrument (USA), following the operating parameters of model S220. The HiSeq X Ten DNA Library Prep Kit for Illumina (Shanghai Yisheng Biotechnology, China) was employed for DNA fragment end repair, ligation junctions, magnetic bead sorting and purification of ligation products, library amplification and purification, and the concentration of the library was determined using a Thermo Qubit 4.0 fluorescence quantification instrument (Thermo Fisher, USA). The constructed library was subjected to paired-end sequencing using next-generation sequencing technology, resulting in the generation of 50,851,778 sequences. We extracted the raw sequences in FASTA format. The raw sequencing data were then processed for quality assessment, data filtering, and counting of valid reads using Fastp 0.36 [21]. Reads with an average quality value lower than Q20 were filtered out before assembly. The percentage of base quality above Q20 was 97.73%. The percentage of clean reads was 99.52% with a total of 50,608,016 reads. The second-generation sequencing data was assembled using SPAdes 3.15 [22]. Using *Carpomya incompleta* as the reference genome, the mitochondrial genome sequence was obtained, with an identical portion of 14,654 bp in length and an average depth of 1148.89-fold. The contig obtained from splicing was patched for gaps using GapFiller1.11 [23]. Sequence corrections were performed using PrInSeS-G to correct base errors and insertion loss of small fragments during

**Table 1**  
The complete mitogenomes used in this study.

No.	Family	Genus	Species	GeneBank No.	Length/bp
1	Tephritidae	<i>Acidiella</i>	<i>Acidiella didymera</i>	MT682536.1	16298
2		<i>Acidiella</i>	<i>Acidiella diversa</i>	NC_053982.1	15531
3		<i>Acrotaeniostola</i>	<i>Acrotaeniostola dissimilis</i>	MH900079.1	15384
4		<i>Anastrepha</i>	<i>Anastrepha fraterculus</i>	NC_034912.1	16739
5		<i>Anastrepha</i>	<i>Anastrepha distincta</i>	NC_071713.1	16977
6		<i>Anastrepha</i>	<i>Anastrepha ludens*</i>	NC_071714.1	16955
7		<i>Anastrepha</i>	<i>Anastrepha obliqua</i>	NC_071715.1	16862
8		<i>Anastrepha</i>	<i>Anastrepha ornata</i>	NC_071716.1	16654
9		<i>Anastrepha</i>	<i>Anastrepha serpentina*</i>	NC_071717.1	16847
10		<i>Anastrepha</i>	<i>Anastrepha striata</i>	NC_071718.1	16962
11		<i>Anastrepha</i>	<i>Anastrepha suspensa</i>	NC_071719.1	16773
12		<i>Bactrocera</i>	<i>Bactrocera albistrigata</i>	MH374118.1	15933
13		<i>Bactrocera</i>	<i>Bactrocera frauenfeldi</i>	MT121261.1	15934
14		<i>Bactrocera</i>	<i>Bactrocera rubigina</i>	MT121270.1	15955
15		<i>Bactrocera</i>	<i>Bactrocera oleae</i>	NC_005333.1	15815
16		<i>Bactrocera</i>	<i>Bactrocera dorsalis*</i>	NC_008748.1	15915
17		<i>Bactrocera</i>	<i>Bactrocera carambolae</i>	NC_009772.1	15915
18		<i>Bactrocera</i>	<i>Bactrocera minax</i>	NC_014402.1	16043
19		<i>Bactrocera</i>	<i>Bactrocera tryoni*</i>	NC_014611.1	15925
20		<i>Bactrocera</i>	<i>Bactrocera correcta</i>	NC_018787.1	15936
21		<i>Bactrocera</i>	<i>Bactrocera zonata</i>	NC_027725.1	15935
22		<i>Bactrocera</i>	<i>Bactrocera arecae</i>	NC_028327.1	15900
23		<i>Bactrocera</i>	<i>Bactrocera latifrons</i>	NC_029466.1	15977
24		<i>Bactrocera</i>	<i>Bactrocera melastomatos</i>	NC_029467.1	15954
25		<i>Bactrocera</i>	<i>Bactrocera umbrosa</i>	NC_029468.1	15898
26		<i>Bactrocera</i>	<i>Bactrocera limbifera</i>	NC_037722.1	15860
27		<i>Bactrocera</i>	<i>Bactrocera ritsemai</i>	NC_037723.1	15927
28		<i>Bactrocera</i>	<i>Bactrocera tsuneonis</i>	NC_038164.1	15865
29		<i>Bactrocera</i>	<i>Bactrocera biguttula</i>	NC_042712.1	15829
30		<i>Bactrocera</i>	<i>Bactrocera ruiliensis</i>	NC_046952.1	15870
31		<i>Bactrocera</i>	<i>Bactrocera thailandica</i>	NC_053983.1	15915
32		<i>Bactrocera</i>	<i>Bactrocera curvifera</i>	NC_071737.1	16152
33		<i>Bactrocera</i>	<i>Bactrocera fulvicauda</i>	NC_071738.1	15935
34		<i>Bactrocera</i>	<i>Bactrocera moluccensis</i>	NC_071739.1	16331
35		<i>Bactrocera</i>	<i>Bactrocera musae</i>	NC_071740.1	16552
36		<i>Bactrocera</i>	<i>Bactrocera nigrotibialis</i>	NC_071741.1	15972
37		<i>Bactrocera</i>	<i>Bactrocera occipitalis</i>	NC_071742.1	15911
38		<i>Bactrocera</i>	<i>Bactrocera tuberculata</i>	NC_071743.1	15937
39		<i>Bactrocera</i>	<i>Bactrocera wuzhishana</i>	NC_071744.1	15942
40		<i>Bactrocera</i>	<i>Bactrocera bryoniae</i>	NC_071745.1	15960
41		<i>Carpomya</i>	<i>Carpomya incompleta</i>	NC_071720.1	16132
42		<i>Carpomya</i>	<i>Carpomya vesuviana*</i>	NC_071721.1	16083
43		<i>Ceratitis</i>	<i>Ceratitis capitata</i>	NC_000857.1	15980
44		<i>Ceratitis</i>	<i>Ceratitis cosyra*</i>	NC_071251.1	15954
45		<i>Ceratitis</i>	<i>Ceratitis quilicii</i>	ON861820.1	16028
46		<i>Ceratitis</i>	<i>Ceratitis rosa*</i>	ON861821.1	15998
47		<i>Dacus</i>	<i>Dacus ciliatus*</i>	MG962405.1	15808
48		<i>Dacus</i>	<i>Dacus longicornis</i>	NC_032690.1	16253
49		<i>Dacus</i>	<i>Dacus conopsoides</i>	NC_043843.1	15852
50		<i>Dacus</i>	<i>Dacus bivittatus*</i>	NC_046468.1	15833
51		<i>Dacus</i>	<i>Dacus trimacula</i>	NC_053984.1	15847
52		<i>Dacus</i>	<i>Dacus vijaysegarani</i>	NC_061932.1	15886
53		<i>Dacus</i>	<i>Dacus armatus</i>	NC_071725.1	15464
54		<i>Dacus</i>	<i>Dacus axanus</i>	NC_071726.1	17494
55		<i>Dacus</i>	<i>Dacus durbanensis</i>	NC_071727.1	16197
56		<i>Dacus</i>	<i>Dacus eclipsis</i>	NC_071728.1	16033
57		<i>Dacus</i>	<i>Dacus humeralis</i>	NC_071729.1	16018
58		<i>Dacus</i>	<i>Dacus venetatus</i>	NC_071730.1	16167
59		<i>Felderimyia</i>	<i>Felderimyia fuscipennis</i>	NC_052851.1	16536
60		<i>Neoceratitis</i>	<i>Neoceratitis asiatica</i>	MF434829.1	15481
61		<i>Philophylla</i>	<i>Philophylla fossata</i>	NC_067084.1	19253
62		<i>Procecidochares</i>	<i>Procecidochares utilis</i>	NC_020463.1	15922
63		<i>Rhagoletis</i>	<i>Rhagoletis cornivora</i>	MN443930.1	14931
64		<i>Rhagoletis</i>	<i>Rhagoletis mendax</i>	MN443939.1	14928
65		<i>Rhagoletis</i>	<i>Rhagoletis zephyria</i>	MN443945.1	14927
66		<i>Rhagoletis</i>	<i>Rhagoletis cerasi</i>	MT121235.1	16428
67		<i>Rhagoletis</i>	<i>Rhagoletis batava</i>	NC_071722.1	16459
68		<i>Rhagoletis</i>	<i>Rhagoletis completa*</i>	NC_071723.1	16406

(continued on next page)

**Table 1** (continued)

No.	Family	Genus	Species	GeneBank No.	Length/bp
69		<i>Rhagoletis</i>	<i>Rhagoletis pomonella</i> *	NC_071724.1	16679
70		<i>Tephritis</i>	<i>Tephritis femoralis</i>	NC_047184.1	15117
71		<i>Zeugodacus</i>	<i>Zeugodacus cucurbitae</i>	MH900082.1	15685
72		<i>Zeugodacus</i>	<i>Zeugodacus scutellatus</i> *	NC_027254.1	15915
73		<i>Zeugodacus</i>	<i>Zeugodacus tau</i> *	NC_027290.1	15687
74		<i>Zeugodacus</i>	<i>Zeugodacus diaphorus</i>	NC_028347.1	15890
75		<i>Zeugodacus</i>	<i>Zeugodacus proprediphora</i>	NC_049063.1	15829
76		<i>Zeugodacus</i>	<i>Zeugodacus cilifer</i>	NC_052852.1	15843
77		<i>Zeugodacus</i>	<i>Zeugodacus caudatus</i>	NC_062801.1	15311
78		<i>Zeugodacus</i>	<i>Zeugodacus mukiae</i>	NC_067083.1	15816
79		<i>Zeugodacus</i>	<i>Zeugodacus atrifacies</i>	NC_071731.1	15876
80		<i>Zeugodacus</i>	<i>Zeugodacus depressus</i>	NC_071732.1	15835
81		<i>Zeugodacus</i>	<i>Zeugodacus diversus</i>	NC_071733.1	15871
82		<i>Zeugodacus</i>	<i>Zeugodacus hochii</i>	NC_071734.1	15850
83		<i>Zeugodacus</i>	<i>Zeugodacus rubellus</i>	NC_071735.1	16332
84		<i>Zeugodacus</i>	<i>Zeugodacus triangularis</i>	NC_071736.1	15859
85	Drosophilidae	<i>Drosophila</i>	<i>Drosophila melanogaster</i>	NC_024511.2	19524
86		<i>Drosophila</i>	<i>Drosophila suzukii</i>	NC_060762.1	16392

Note: (\*) designate the 13 Tephritidae species used in the AT base content and AT/GC skew analyses.

splicing.

### 2.3. Sequence annotation and analysis

The base content and AT/GC skew of each section of the mitochondrial genomes of *C. pardalina* as well as of 13 other species of the Tephritidae family (Table 1), were counted using the software PhyloSuite\_v1.2.3. Additionally, the relative synonymous codon usage (RSCU) was analyzed, and RSCU histograms were generated. CDS gene boundaries were obtained using tblastn with genewise for reverse blast with the reference genome. MiTFi was used for tRNA sequence annotation, and cmssearchfam was used for identifying noncoding rRNAs [24]. The online software tRNAscan-SE (<http://lowelab.ucsc.edu/tRNAscan-SE>) was utilized for secondary structure prediction of tRNAs. Any unsuccessfully predicted secondary structure structures were manually mapped [25].

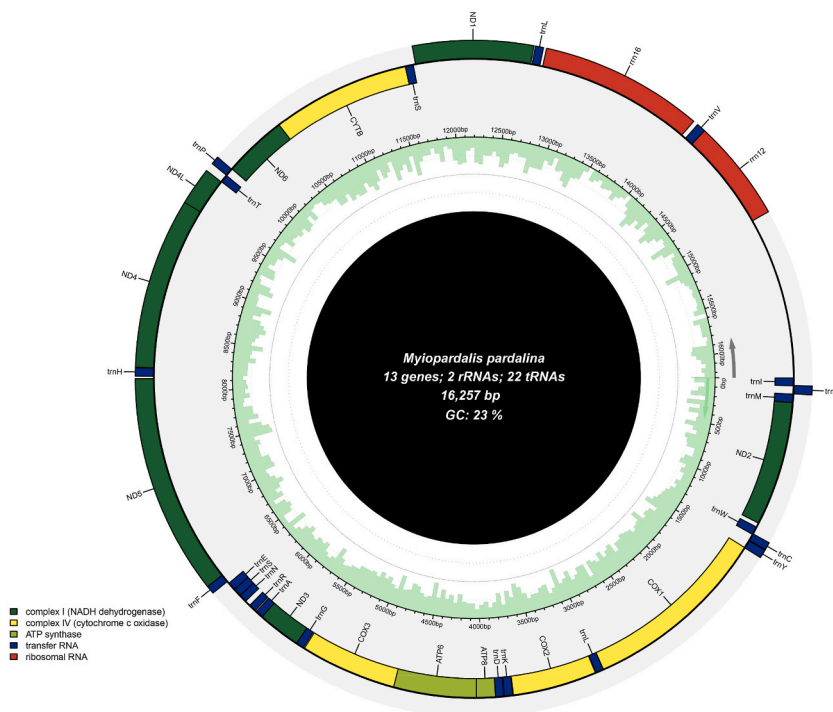


**Fig. 1.** Mitochondrial genome structure of *Carpomya pardalina*. Note: The inner circle data indicates the GC% of the corresponding position.

## 2.4. Phylogenetic analysis

The mitochondrial genome sequences of 84 species, belonging to 14 genera including *Anastrepha*, *Bactrocera*, *Carpomya*, *Ceratitis*, *Dacus*, and *Rhagoletis*, were downloaded from the GeneBank of the National Center for Biotechnology Information (NCBI). The species used in this study are listed in Table 1, along with their respective details.

The Extract function in Phylosuite v1.2.3 [26] was utilized to extract 13 PCGs and 2 rRNAs. The multiple sequence alignment of the 13 PCGs was performed using the G-INS-i strategy in MAFFT [27], and the sequence alignment results were then optimized using MACSE [28]. Gblocks was utilized for sequence pruning of the PCGs sequences [29]. The RNA sequences were trimmed using trimAl [30]. The corresponding sequences were concatenated to generate two datasets using the Concatenate Sequences function: 1) 13 PCGs; 2) 13 PCGs + 2rRNA.

PartitionFinder 2 was utilized to predict the optimal model for each dataset. The “greedy” algorithm and AICc standard were used to determine the optimal partitioning strategy and the best alternative model for each partition [31]. For this study, maximum likelihood (ML) and Bayesian inference (BI) were employed to construct phylogenetic trees using the two datasets. ML trees were constructed using IQ-Tree [32], and the support values of each node were estimated using the rapid bootstrap algorithm with 10,000 replicates [33]. BI trees were constructed using MrBayes, running 4 Markov chains (MCMC) for a total of  $2 \times 10^7$  generations, sampled every 1000 generations [34]. Default settings were used for the remaining parameters. Burnin is used to discard the first 25% of the trees, and the remaining trees were used to calculate the consensus tree and evaluate the posterior probability of branches. The ML and BI trees generated from the two datasets were visualized and edited using the iTOL online website (<https://itol.embl.de/>).

## 3. Result and discussion

### 3.1. Mitochondrial genome structure and base composition

The mitochondrial genome of *C. pardalina* has a length of 16,257 bp (Accession number: OR387322). It possesses a closed circular

**Table 2**  
Gene organization of the mitochondrial genome of *Carpomya pardalina*.

Genes	Coding strand	Position(bp)	Gene length(bp)	Start codon	Stop codon	Anticodon	Intergenic length(bp)
<i>tRNA<sup>Ile(I)</sup></i>	J	1–65	65			GAT	–3
<i>tRNA<sup>Gln(Q)</sup></i>	N	63–131	69			TTG	1
<i>tRNA<sup>Met(M)</sup></i>	J	133–201	69			CAT	0
<i>ND2</i>	J	202–1224	1023	ATT	TAA		35
<i>tRNA<sup>Trp(W)</sup></i>	J	1260–1327	68			TCA	–8
<i>tRNA<sup>Cys(C)</sup></i>	N	1320–1381	62			GCA	4
<i>tRNA<sup>Tyr(Y)</sup></i>	N	1386–1452	67			GTA	–2
<i>COX1</i>	J	1451–2984	1534	TCG	T		0
<i>tRNA<sup>Leu(L)</sup></i>	J	2985–3050	66			TAA	4
<i>COX2</i>	J	3055–3742	688	ATG	T		3
<i>tRNA<sup>Lys(K)</sup></i>	J	3746–3816	71			CTT	3
<i>tRNA<sup>Asp(D)</sup></i>	J	3820–3887	68			GTC	0
<i>ATP8</i>	J	3888–4049	162	ATT	TAA		–7
<i>ATP6</i>	J	4043–4720	678	ATG	TAA		–1
<i>COX3</i>	J	4720–5508	789	ATG	TAA		9
<i>tRNA<sup>Gly(G)</sup></i>	J	5518–5583	66			TCC	0
<i>ND3</i>	J	5584–5937	354	ATT	TAG		–2
<i>tRNA<sup>Ala(A)</sup></i>	J	5936–6000	65			TGC	10
<i>tRNA<sup>Arg(R)</sup></i>	J	6011–6073	63			TCG	46
<i>tRNA<sup>Asn(N)</sup></i>	J	6120–6185	66			GTT	0
<i>tRNA<sup>Ser(S)</sup></i>	J	6186–6254	69			GCT	0
<i>tRNA<sup>Glu(E)</sup></i>	J	6255–6321	67			TTC	18
<i>tRNA<sup>Phe(F)</sup></i>	N	6340–6405	66			GAA	0
<i>ND5</i>	N	6406–8122	1717	ATT	T		18
<i>tRNA<sup>His(H)</sup></i>	N	8141–8205	65			GTG	3
<i>ND4</i>	N	8209–9549	1341	ATG	TAG		–7
<i>ND4L</i>	N	9543–9839	297	ATG	TAG		2
<i>tRNA<sup>Thr(T)</sup></i>	J	9842–9906	65			TGT	0
<i>tRNA<sup>Pro(P)</sup></i>	N	9907–9972	66			TGG	2
<i>ND6</i>	J	9975–10499	525	ATT	TAA		–1
<i>CYTB</i>	J	10499–11635	1137	ATG	TAG		–2
<i>tRNA<sup>Ser(S)</sup></i>	J	11634–11700	67			TGA	18
<i>ND1</i>	N	11719–12655	937	ATA	T		10
<i>tRNA<sup>Leu(L)</sup></i>	N	12666–12730	65			TAG	23
<i>16S rRNA</i>	N	12754–14023	1270				38
<i>tRNA<sup>Val(V)</sup></i>	N	14062–14133	72			TAC	–1
<i>12S rRNA</i>	N	14133–14926	794				0
Control region		14927–16257	1331				0

double-stranded molecular structure, containing two genes encoding ribosomal RNAs (rRNAs), 22 genes encoding transfer RNAs (tRNAs), 13 protein-coding genes (PCGs), and a control region (Fig. 1). The order of the 37 genes in the mitochondrial genome of *C. pardalina* is provided in Table 2. Among the 13 PCGs, *COX1*, *COX2*, *COX3*, *ATP6*, *ATP8*, *NAD2*, *NAD3*, *NAD6*, and *CYTB* were located in the J strand, while the remaining four were located on the N strand. Among the 22 tRNA genes, *tRNA<sup>Ile(I)</sup>*, *tRNA<sup>Met(M)</sup>*, *tRNA<sup>Trp(W)</sup>*, *tRNA<sup>Leu(L)</sup>*, *tRNA<sup>Lys(K)</sup>*, *tRNA<sup>Asp(D)</sup>*, *tRNA<sup>Gly(G)</sup>*, *tRNA<sup>Ala(A)</sup>*, *tRNA<sup>Arg(R)</sup>*, *tRNA<sup>Asn(N)</sup>*, *tRNA<sup>Ser(S)</sup>*, *tRNA<sup>Glu(E)</sup>*, *tRNA<sup>Thr(T)</sup>*, and *tRNA<sup>Ser(S)</sup>* were located on the J strand, while the remaining eight were located on the N strand. The two rRNA genes were located on the N strand. The AT control region, which was 1,331bp long, was positioned between *12S rRNA* and *tRNA<sup>Ile(I)</sup>* genes. It exhibited a high AT content of 85.05%.

The mitochondrial genome of *C. pardalina* exhibited a total of ten gene overlaps, spanning 34 bp. The longest overlap was observed between *tRNA<sup>Trp(W)</sup>* and *tRNA<sup>Cys(C)</sup>*, with a sequence overlap of 8 bp. Additionally, 18 spacer regions were identified in the mitochondrial genome, comprising a total of 247 bp. The longest spacer, measuring 46 bp in length, was located between *tRNA<sup>Arg(R)</sup>* and *tRNA<sup>Asn(N)</sup>*. Furthermore, there were ten regions without any overlap or spacer (Table 2). These findings are consistent with the published mitochondrial genomes of other Tephritidae species [35–38].

The compositions of A, T, G and C in the mitochondrial genome of *C. pardalina* were 40.36%, 36.32%, 9.61%, and 13.70%, respectively, with the highest content of A and the lowest content of G (Table 3). The overall mitochondrial genome, including the two rRNAs, 22 tRNAs, 13 PCGs, and control region of *C. pardalina*, displayed a high A + T content ranging from 74.91% to 85.05%. This indicates a significant bias towards A and T bases. This observation is consistent with the published mitochondrial genome data of other Tephritidae species (Fig. 2). The A + T content bias in the insect mitochondrial genome is a well-known characteristic, with an AT skew of 0.053 and a GC skew of −0.175. These values suggest a genome-wide preference for A and C bases [39–41]. In a study conducted by Wei et al., in 2010, the base preferences of 120 insect mitochondrial genomes, and the results showed that the relative content of base G + C was related to the replication direction of the mitochondrial genome, rather than the gene direction. On the other hand, the relative content of base A + T was related to gene direction, replication and codon positions. These findings highlight the complex relationship between base composition and various factors influencing the organization and function of insect mitochondrial genomes.

Therefore, the investigation of base composition preference holds great significance in understanding gene replication and transcription mechanism [42]. Among the thirteen PCGs, the *COX1* and *COX3* genes exhibited the lowest AT content, while the *ATP8* and *NAD6* genes had the highest AT content. The *COX1* gene is known to be a highly conserved mitochondrial gene in animals and can serve as a barcode for species identification, determining inter- and intra-species differences, and other applications in insect identification [43–45]. The relatively higher GC content in these genes helps reduce the mutation rate and maintain genetic stability [46, 47]. The AT skew was found to be negative for all 13 PCGs. Nine PCGs located on the J strand exhibited negative GC skews, while the four PCGs on the N strand had positive GC skew. The two rRNA genes displayed positive GC skew as well. These observations are consistent with the AT/GC skew patterns observed in the majority of Tephritidae mitochondrial genomes (Fig. 3) [35–37].

### 3.2. Protein-coding genes

The arrangement of PCGs in the mitochondria of *C. pardalina* is consistent with that observed in other Tephritidae insect [35–37]. The combined length of the 13 PCGs in *C. pardalina* is 11,182 bp, which accounts for 68.78% of the total length of the mitochondrial genome. The longest gene is *ND5* on the N strand with a sequence length of 1717 bp, while the shortest gene is *ATP8* on the J strand with a length of 162 bp. The start codon for the *COX1* gene is TCG, while the remaining 12 PCGs have ATN as the start codon. *ND1* has

**Table 3**  
Nucleotide composition of the mitochondrial genome of *Carpomya pardalina*.

Gene	A/%	T/%	G/%	C/%	A + T/%	G + C/%	AT-skew	GC-skew
Whole genome	40.36	36.32	9.61	13.70	76.69	23.31	0.053	−0.175
13PCGs	31.60	43.30	12.93	12.16	74.91	25.09	−0.156	0.031
22tRNAs	37.63	39.20	13.29	9.88	76.82	23.18	−0.020	0.147
2rRNAs	36.82	42.54	13.03	7.61	79.36	20.64	−0.072	0.263
Control region	45.15	39.89	5.33	9.62	85.05	14.95	0.062	−0.286
16S rRNA	37.01	43.62	12.52	6.85	80.63	19.37	−0.082	0.293
12S rRNA	36.52	40.81	13.85	8.82	77.33	22.67	−0.055	0.222
ND2	34.70	44.18	8.70	12.41	78.89	21.11	−0.120	−0.176
COX1	31.16	38.14	15.06	15.65	69.30	30.70	−0.101	−0.019
COX2	35.90	36.63	12.35	15.12	72.53	27.47	−0.010	−0.101
ATP8	40.74	41.98	6.17	11.11	82.72	17.28	−0.015	−0.286
ATP6	32.15	41.45	10.62	15.78	73.60	26.40	−0.126	−0.196
COX3	30.80	38.78	14.96	15.46	69.58	30.42	−0.115	−0.017
ND3	33.62	44.63	9.60	12.15	78.25	21.75	−0.141	−0.117
ND5	29.70	47.76	14.33	8.21	77.46	22.54	−0.233	0.271
ND4	28.93	48.02	14.17	8.87	76.96	23.04	−0.248	0.230
ND4L	27.61	51.52	14.14	6.73	79.12	20.88	−0.302	0.355
ND6	40.19	42.10	6.86	10.86	82.29	17.71	−0.023	−0.226
CYTB	32.98	38.43	12.75	15.83	71.42	28.58	−0.076	−0.108
ND1	25.83	49.63	15.80	8.75	75.45	24.55	−0.315	0.287

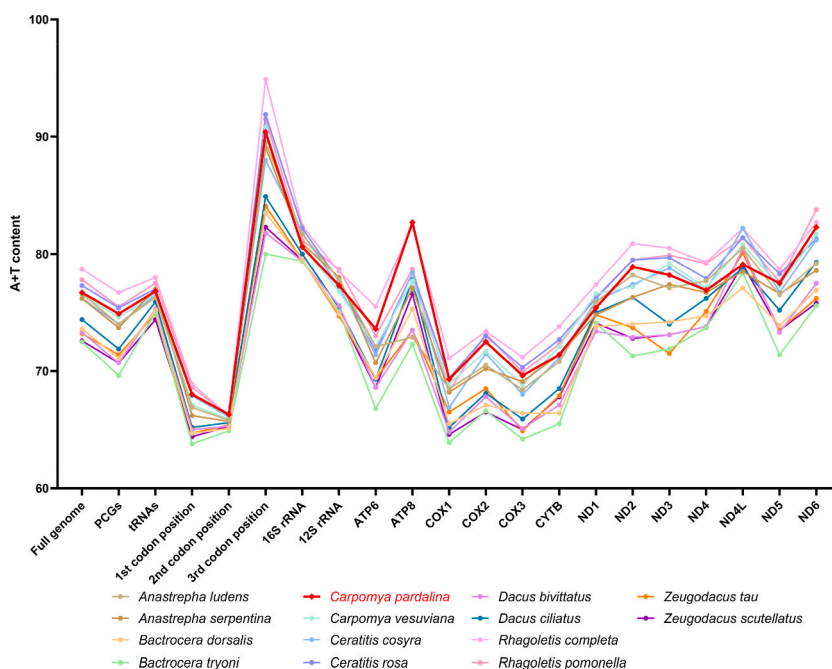


**Fig. 2.** A + T content of individual elements and the complete genome in 14 species of Tephritidae.

ATA as the start codon, *ND2*, *ND3*, *ND5*, *ND6*, and *ATP8* have ATT as the start codon, and *COX2*, *COX3*, *ATP6*, *ND4*, *ND4L*, and *CYTB* have ATG as the start codon. The termination codon for *ND3*, *ND4*, and *CYTB* is TAG. *ND2*, *ND4L*, *ND6*, *ATP8*, *ATP6*, and *COX3* have TAA as the termination codon, while *COX1*, *COX2*, *ND5*, and *ND1* terminate with an incomplete termination codon T. This is similar to other Tephritidae mitochondrial genomes [35–37], where the full termination codon TAA is completed by post-transcriptional polyadenylation, which adds extra A to the incomplete termination codon [48]. Additionally, there are overlapping regions between certain PCGs, with a 7 bp overlap between *ATP6* and *ATP8* genes, a 1 bp overlap between *ATP6* and *COX3* genes, a 7 bp overlap between *ND4L* and *ND4* genes, and a 1 bp overlap between *CYTB* and *ND6* genes (Table 2).

The relative synonymous codon usage (RSCU) of the mitochondrial PCGs in *C. pardalina* and 13 other Tephritidae species is shown in Fig. 4. Among all 14 species, the most abundant codon families were Leu2, Ile, and Phe, which exhibited a strong preference for AT-rich codons (as shown in Fig. 4). This pattern is similar to what has been observed in Lepidoptera, Tetraonchoidea and Nemertea [49–51].

In the PCGs of *C. pardalina*, the codon with the highest RSCU value was UUA, with an RSCU value of 4.44. Conversely, the codon with the lowest frequency was CUC, with an RSCU value of only 0.04. The RSCU values of various codons exhibited considerable variation, indicating a significant bias in codon frequency within the mitochondrial genome of *C. pardalina*. The codons with the highest frequency predominantly consisted of A and T base, which could be attributed to the higher abundance of AT bases compared to GC bases in the PCGs sequences of *C. pardalina*. The third codon position of PCGs generally contains more AT bases than the first and second codon positions (as shown in Fig. 2), resulting in a higher usage of codons ending in A or U. This phenomenon is a common feature observed in Metazoa [51–53].

### 3.3. Transfer RNAs and ribosomal RNAs

Similar to other Tephritidae insects, *C. pardalina* possesses a set of 22 tRNAs. Among these 22 RNAs, the longest is 72 bp, while the shortest one is 62 bp in length. Predicted secondary structures of all 22 tRNAs in *C. pardalina* exhibit the typical cloverleaf structures (as shown in Fig. 5). In the secondary structures of tRNAs from Tephritidae insects, base pair mismatches are commonly observed [35–37]. For instance, *Bactrocera biguttula* has 32 base pair mismatches [36], *Bactrocera tsuneonis* has 30 base pair mismatches [37], and *C. pardalina* has 21 G-U mismatches in the predicted structures of its 22 tRNAs.

These mismatched bases can be corrected through post-transcriptional editing and do not affect the function of tRNA genes [54,55]. Among the mismatches, there are 10 pairs on the DHU arm, 1 pair on the anticodon arm, 8 pairs on the amino acid acceptor arm, and 2 pairs on TΨC. A slight preference for T nucleotides was observed in the tRNA ligation of the *C. pardalina* mitochondrial genome (AT skew,  $-0.02$ ), which is consistent with the preference for T nucleotides observed in other analyzed Tephritidae species (as shown in Fig. 3).

Both of the rRNAs in the mitochondrial genome of *C. pardalina* are located on the N strand. The *16S rRNA* is positioned between *tRNA<sup>Leu(L)</sup>* and *tRNA<sup>Val(V)</sup>*, while the *12S rRNA* is located between *tRNA<sup>Val(V)</sup>* and the control region. The length of the *16S rRNA* is 1270 bp, which is longer than the *12S rRNA* that spans 794 bp. The A + T content of the *16S rRNA* is 80.63%, while the *12S rRNA* has a

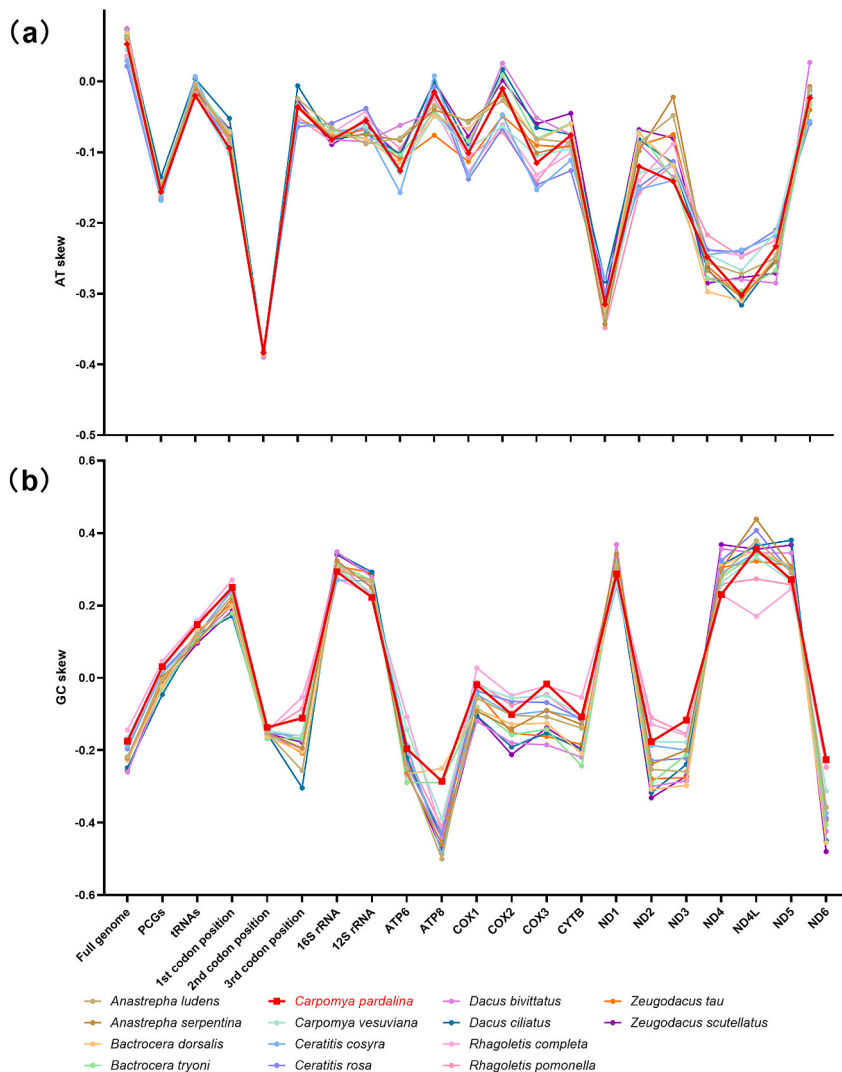


**Fig. 3.** (a) AT skew and (b) GC skew of individual elements and the complete genome in 14 species of Tephritidae.

slightly lower A + T content of 70.33%. The AT skew of the *16S rRNA* is  $-0.082$ , indicating a preference for T bases among the AT bases. Similarly, the AT skew of the *12S rRNA* is  $-0.055$  suggesting a preference for T bases as well (as shown in [Tables 2 and 3](#)).

### 3.4. Phylogenetic analysis

For phylogenetic analysis, *Drosophila melanogaster* and *Drosophila suzukii* were selected as outgroup species, while *Neoceratitis*, *Dacus*, *Bactrocera*, *Acrotaeniostola*, *Rhagoletis*, *Acidiella*, *Ceratitis*, *Procecidochares*, *Drosophila*, and *Zeugodacus*, *Anastrepha*, *Tephritis*, *Felderimyia*, *Philophylla*, and *Carpomya*, comprising a total of 85 species from 15 families, were used as ingroup species. The two datasets used for phylogenetic analysis are as follows: 1) 13 PCGs and 2 rRNAs: 13,204 nucleotides; 2) 13 PCGs: 11,115 nucleotides. The molecular phylogeny of *C. pardalina* in relation to other Tephritidae species was constructed using the two datasets mentioned above. The resulting phylogenetic tree is presented in [Fig. 6](#). Both Bayesian inference (BI) and maximum likelihood (ML) analyses generated two trees with similar topologies. However, the node support values varied slightly between the two methods, with the BI tree generally exhibiting higher node support than the ML tree. This difference in node support values is commonly observed in phylogenetic studies [[56,57](#)].

All four trees generated from the two datasets showed that *C. pardalina* clustered in the genus *Carpomya*, which aligns with traditional morphological taxonomic findings [[5](#)]. *C. pardalina* was found to be closely related to *Carpomya incompleta* and *Carpomya vesuviana*, forming a sister group with them. Additionally, the *Carpomya* genus and the *Rhagoletis* genus were identified as sister groups in the phylogenetic analysis. This finding is consistent with a previous study conducted by Zhang et al. [[8](#)]. In that study, four phylogenetic trees were constructed using two datasets, and the results also supported that *Ceratitis*, *Anastrepha*, *Carpomya*, *Rhagoletis*,



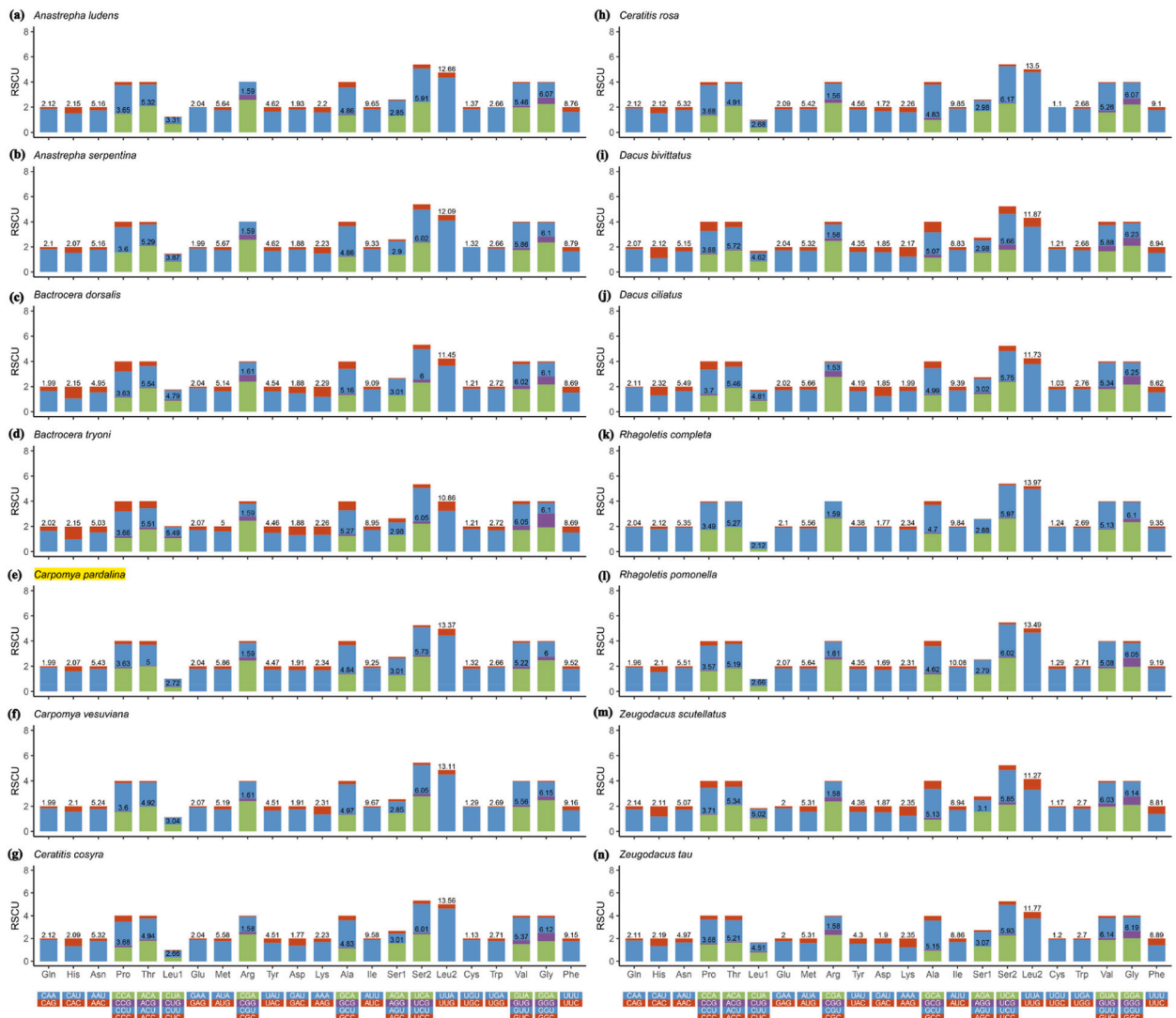


**Fig. 4.** Relative synonymous codon usage in the mitogenome of *Carpomya pardalina* (e) and 13 other Tephritidae species. (a)*Anastrepha ludens*; (b) *Anastrepha serpentina*; (c)*Bactrocera dorsalis*; (d)*Bactrocera tryoni*; (f)*Carpomya pardalina*; (g)*Ceratitis cosyra*; (h)*Ceratitis rosa*; (i)*Dacus ciliatus*; (j) *Dacus bivittatus*; (k)*Rhagoletis completa*; (l)*Rhagoletis pomonella*; (m)*Zeugodacus scutellatus*; (n)*Zeugodacus tau*  
 Note: Codon families were indicated below the X-axis. Values on the top of the bars denote amino acid usage.

*Dacus* and *Bactrocera* were monophyletic groups. *Zeugodacus* is the monophyletic group in Fig. 6-A. *Zeugodacus cilifer* is sister to other species of *Zeugodacus* and *Dacus*, and *Zeugodacus* is not monophyletic in Fig. 6-B, C, and D. In other studies, the genus *Zeugodacus* was shown to be a monophyletic group, sister to *Dacus*, and clustered with *Bactrocera* [35–37,58]. It is worth noting that these results may vary due to different datasets, tree-building methods, and evolutionary models employed. Therefore, further support from additional data is needed to confirm these relationships.

In addition, there are differences in the evolutionary rates of the first, second and third codon position due to codon degeneracy, and the combined analysis of these differences may have implications for the stability of inferred phylogenetic relationships. The effect of the third codon on inferring phylogenetic relationships was not assessed in this study, which is a shortcoming of this study. However, this study focuses on the phylogenetic relationships of the *Carpomya* genus within the family Tephritidae, and all four phylogenetic trees produced the same results for the *Carpomya* genus. In the future, when studying the phylogenetic relationship of the entire Tephritidae family, more mitochondrial genome data can be added and more datasets can be selected for analysis.

**4. Conclusions**

In summary, we conducted high-throughput sequencing to sequence and analyze the mitochondrial genome of *C. pardalina*. Our analysis shed light on the taxonomic position of *C. pardalina* within the Tephritidae family. The phylogenetic trees constructed using

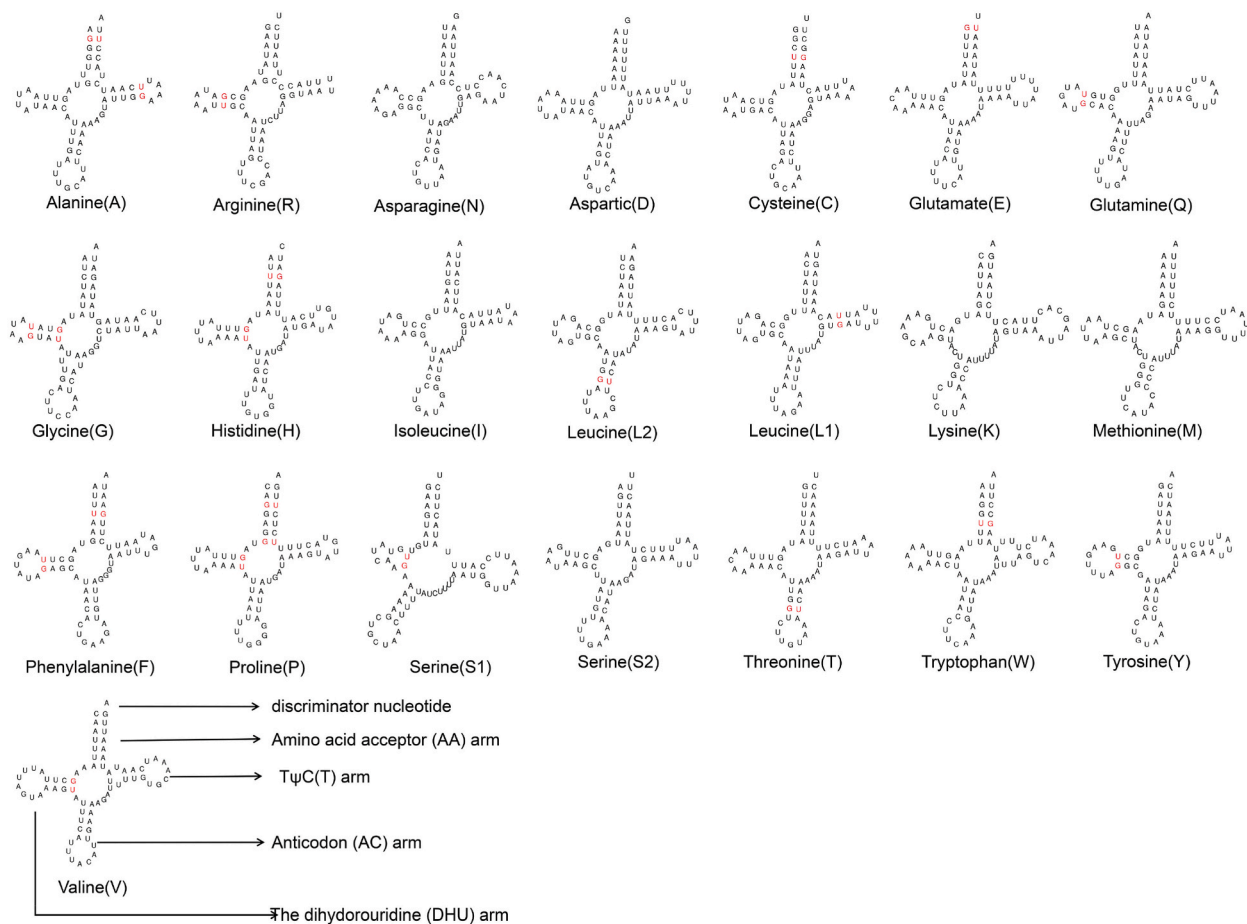


**Fig. 5.** Predicted secondary structures of tRNA genes in mitogenome of *Carpomyia pardalina*.

the two datasets consistently placed *C. pardalina* in the genus *Carpomyia*, supporting the findings of traditional morphological taxonomy. Additionally, *C. pardalina* was found to have a sister relationship with the evolutionary branch comprising *C. incompleta* and *C. vesuviana*. The availability of the complete mitochondrial genome of *C. pardalina* is valuable for future studies on molecular characterization, population genetics, and molecular phylogenetics of the Tephritidae family.

## Funding

This work was supported by the Major Science and Technology Projects in Xinjiang, China (2023A02006).

## Data availability statement

The datasets generated during the current study are available in the National Center for Biotechnology Information at <https://www.ncbi.nlm.nih.gov>. Accession numbers is: OR387322.

## CRedit authorship contribution statement

**Xianting Guo:** Writing – original draft, Software, Methodology, Data curation. **Hualing Wang:** Software, Methodology. **Kaiyun Fu:** Resources, Investigation. **Xinhua Ding:** Resources, Investigation. **Jianyu Deng:** Writing – review & editing, Funding acquisition, Conceptualization. **Wenchao Guo:** Project administration, Investigation, Funding acquisition. **Qiong Rao:** Writing – review & editing, Supervision, Methodology, Data curation, Conceptualization.

## Declaration of competing interest

The authors declare the following financial interests/personal relationships which may be considered as potential competing interests: Qiong Rao reports financial support was provided by Zhejiang A and F University. If there are other authors, they declare that

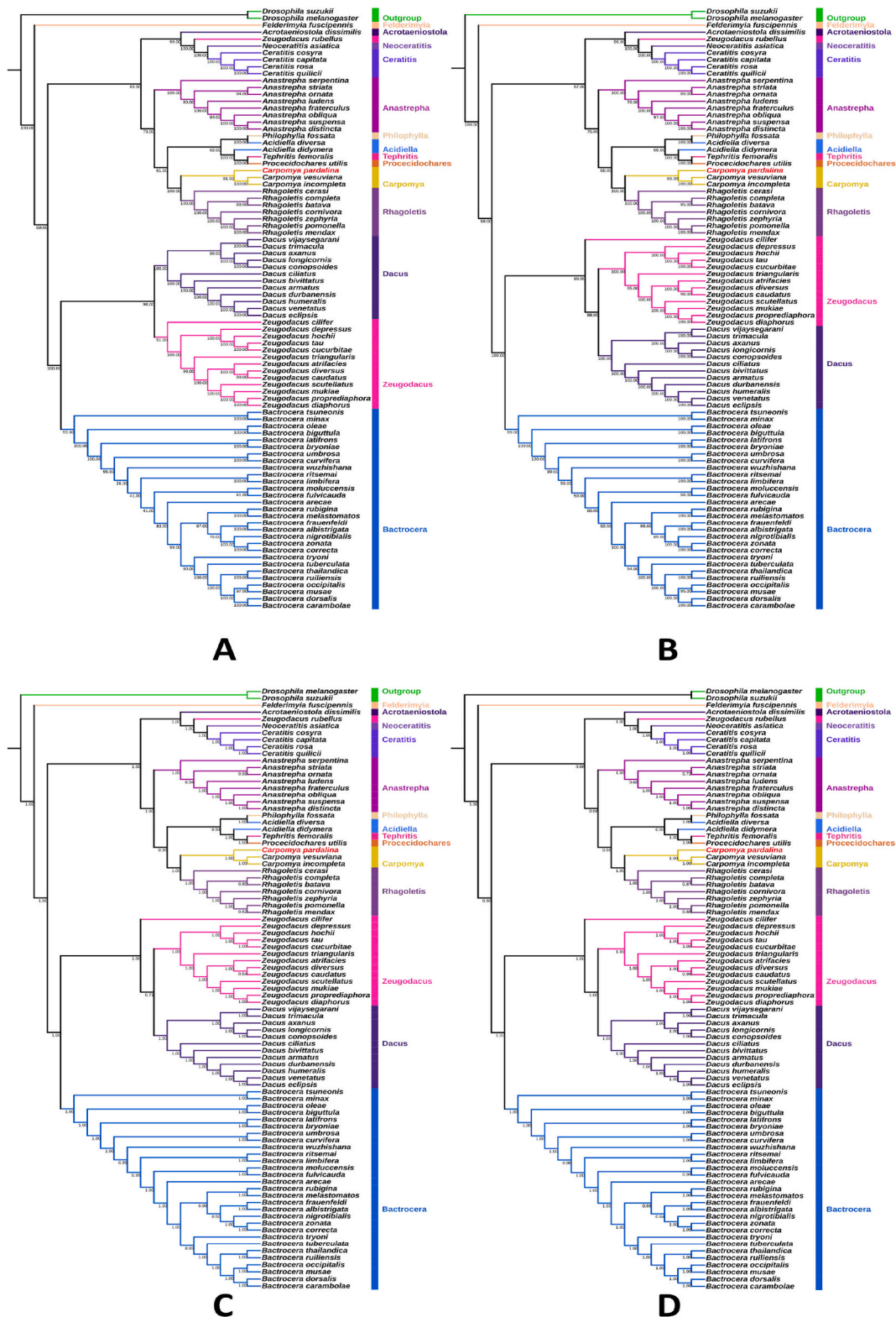


Fig. 6. Maximum Likelihood (ML) and Bayesian inference (BI) phylogenetic trees inferred from mitochondrial genomes of Tephritidae based on two datasets. (A) ML- 13 PCGs and 2 rRNAs; (B) ML- 13 PCGs; (C) BI- 13 PCGs and 2 rRNAs; (D) BI- 13 PCGs; Values above the nodes represent bootstrap values or Bayesian posterior probabilities.

they have no known competing financial interests or personal relationships that could have appeared to influence the work reported in this paper.

## References

- [1] J. Stonehouse, S.M. Sadeed, A. Harvey, et al., *Myiopardalis pardalina* in Afghanistan. Proceedings of the 7th International Symposium on Fruit Flies of Economic Importance, 2006, pp. 1–15.
- [2] E. Bayhan, S. Ölmez Bayhan, Distribution and infestation rate melon fly (*Myopardalis pardalina* (Dip: tephritidae) in Diyarbakır (Turkey). The 3rd International Symposium on EuroAsian Biodiversity, 2017, p. 27.
- [3] A. Baris, S. Cobanoglu, Investigation on the biology of melon fly [*Myiopardalis pardalina* (Bigot, 1891) (Diptera: tephritidae)] in ankara province, Turkish J. Entomol. 37 (3) (2013) 293–304.
- [4] F. Ullah, A.U. Andar, H. Badshah, M. Younus, Management of melon fruit fly (*Myopardalis pardalina* Bigot) in Badghis, Afghanistan, J. Entomol. Zool. Stud. 24 (34) (2015), <https://doi.org/10.1080/09670878709371110>, 24–27.
- [5] B.B.T.Y. Zhunussova, Quarantine protective measures against the melon flies (*Myiopardalis pardalina* Bigot) in Kazakhstan, Online J. Biol. Sci. 17 (4) (2017).
- [6] C.G. Huang, J.C. Hsu, D.S. Haymer, G.C. Lin, W.J. Wu, Rapid identification of the mediterranean fruit fly (Diptera: tephritidae) by loop-mediated isothermal amplification, J. Econ. Entomol. 102 (3) (2009) 1239–1246, <https://doi.org/10.1603/029.102.0350>.
- [7] M.J. Blacket, A. Agarwal, L. Zheng, J.P. Cunningham, B.C. Rodoni, A lamp assay for the detection of *Bactrocera tryoni* Queensland fruit fly (Diptera: Tephritidae), Sci. Rep. 10 (1) (2020) 9554, <https://doi.org/10.1038/s41598-020-65715-5>.
- [8] Y. Zhang, H. Li, S. Feng, Y. Qin, M. De Meyer, M. Virgilio, S. Singh, F. Jiang, A.P. Kawi, A. Susanto, I. Martinez-Sañudo, J. Wu, K. Badji, U. Davaasambu, Z. Li, Mitochondrial phylogenomics reveals the evolutionary and biogeographical history of fruit flies (Diptera: Tephritidae), Entomol. Gen. 43 (2) (2022) 359–368, <https://doi.org/10.1127/entomologia/2022/1594>.
- [9] S.J. Wei, X.X. Chen, Progress in research on the comparative mitogenomics of insects, Chin. J. Appl. Entomol. 48 (6) (2009) 1573–1585, <https://doi.org/10.3724/SP.J.1011.2011.00150>.
- [10] X. Liang, P. Wang, L. Zhang, Z. Li, Y. Xiao, Determining the complete mitochondrial genome of *Tethea albicostata* (Lepidoptera: Drepanidae) and phylogenetic analysis, Mitochondrial DNA B Resour 8 (9) (2023) 963–966, <https://doi.org/10.1080/23802359.2023.2254462>.
- [11] S.C. Chen, H.Y. Jiang, S.R. Liao, T.X. Chen, X.Q. Wang, Complete mitochondrial genome of *Stethoconus japonicus* (Hemiptera: Miridae): insights into the evolutionary traits within the family Miridae, Gene 891 (2024) 147830, <https://doi.org/10.1016/j.gene.2023.147830>.
- [12] C.Y. Su, D.H. Zhu, Y. Abe, T. Ide, Z. Liu, The complete mitochondrial genome and gene rearrangements in a gall wasp species, *Dryocosmus liui* (Hymenoptera: Cynipoidea: Cynipidae), PeerJ 11 (2023) e15865, <https://doi.org/10.7717/peerj.15865>.
- [13] S.H. Wang, S.Y. Hu, M. Li, M. Liu, H. Sun, J.R. Zhao, W.T. Chen, M.L. Yuan, Comparative mitogenomic analyses of darkling beetles (Coleoptera: Tenebrionidae) provide evolutionary insights into tRNA-like sequences, Genes 14 (9) (2023) 1738, <https://doi.org/10.3390/genes14091738>.
- [14] Y.C. Qin, J. Liu, X.D. Li, Y.Z. Chen, W.A. Deng, On the specific status of *Scelimenaspicupennis* and a new record of *S. discalis* from China with mitochondrial genome characterization (Orthoptera, Tetrigridae), ZooKeys 1185 (2023) 83–104, <https://doi.org/10.3897/zookeys.1185.110148>.
- [15] A. Mukherjee, A. Ghosh, K. Tyagi, V. Kumar, D. Banerjee, A. Naskar, Characterization of complete mitochondrial genome of three Horse flies of the genus *Tabanus* (Diptera: Tabanidae): comparative analysis, Mol. Biol. Rep. 50 (12) (2023) 9897–9908, <https://doi.org/10.1007/s11033-023-08837-z>.
- [16] J. Alcolado, Power, sex, suicide: mitochondria and the meaning of life, BMJ 331 (7520) (2005) 851.
- [17] J.L. Boore, Animal mitochondrial genomes, Nucleic Acids Res. 27 (8) (1999) 1767–1780, <https://doi.org/10.1093/nar/27.8.1767>.
- [18] S.L. Cameron, Insect mitochondrial genomics: implications for evolution and phylogeny, Annu. Rev. Entomol. 59 (2014) 95–117, <https://doi.org/10.1146/annurev-ento-011613-162007>.
- [19] H. Chang, J. Guo, M. Li, Y. Gao, S. Wang, X. Wang, Y. Liu, Comparative genome and phylogenetic analysis revealed the complex mitochondrial genome and phylogenetic position of *Conopomorpha sinensis* Bradley, Sci. Rep. 13 (1) (2023) 4989, <https://doi.org/10.1038/s41598-023-30570-7>.
- [20] S. Bi, Y. Song, L. Liu, J. Wan, Y. Zhou, Q. Zhu, J. Liu, Complete mitochondrial genome of *Piophilha casei* (Diptera: Piophilidae): genome description and phylogenetic implications, Genes 14 (4) (2023), <https://doi.org/10.3390/genes14040883>.
- [21] S. Chen, Y. Zhou, Y. Chen, J. Gu, fastp: an ultra-fast all-in-one FASTQ preprocessor, Bioinformatics 34 (17) (2018) 1884–1890, <https://doi.org/10.1093/bioinformatics/bty560>.
- [22] A. Bankevich, S. Nurk, D. Antipov, A.A. Gurevich, M. Dvorkin, A.S. Kulikov, V.M. Lesin, S.I. Nikolenko, S. Pham, A.D. Pribelski, A.V. Pyshkin, A.V. Sirotkin, N. Vyahhi, G. Tesler, M.A. Alekseyev, P.A. Pevzner, SPAdes: a new genome assembly algorithm and its applications to single-cell sequencing, J. Comput. Biol. 19 (5) (2012) 455–477, <https://doi.org/10.1089/cmb.2012.0021>.
- [23] M. Boetzer, W. Pirovano, Toward almost closed genomes with GapFiller, Genome Biol. 13 (6) (2012) R56, <https://doi.org/10.1186/gb-2012-13-6-r56>.
- [24] S.F. Altschul, T.L. Madden, A.A. Schäffer, J. Zhang, Z. Zhang, W. Miller, D.J. Lipman, Gapped BLAST and PSI-BLAST: a new generation of protein database search programs, Nucleic Acids Res. 25 (17) (1997) 3389–3402, <https://doi.org/10.1093/nar/25.17.3389>.
- [25] P.P. Chan, T.M. Lowe, tRNAscan-SE: searching for tRNA genes in genomic sequences, Methods Mol. Biol. 1962 (2019) 1–14, <https://doi.org/10.1007/978-1-4939-9173-01>.
- [26] C. Xiang, F. Gao, I. Jakovčić, H. Lei, Y. Hu, H. Zhang, H. Zou, G. Wang, D. Zhang, Using phylsuite for molecular phylogeny and tree-based analyses, iMeta 2 (1) (2023) e87, <https://doi.org/10.1002/imt2.87>.
- [27] K. Katoh, D.M. Standley, MAFFT multiple sequence alignment software version 7: improvements in performance and usability, Mol. Biol. Evol. 30 (4) (2013) 772–780, <https://doi.org/10.1093/molbev/mst010>.
- [28] V. Ranwez, E. Douzery, C. Cambon, N. Chantret, F. Delsuc, Macse v2: toolkit for the alignment of coding sequences accounting for frameshifts and stop codons, Mol. Biol. Evol. 35 (10) (2018) 2582–2584, <https://doi.org/10.1093/molbev/msy159>.
- [29] G. Talavera, J. Castresana, Improvement of phylogenies after removing divergent and ambiguously aligned blocks from protein sequence alignments, Syst. Biol. 56 (4) (2007) 564–577, <https://doi.org/10.1080/10635150701472164>.
- [30] S. Capella-Gutierrez, J.M. Silla-Martinez, T. Gabaldon, Trimal: a tool for automated alignment trimming in large-scale phylogenetic analyses, Bioinformatics 25 (15) (2009) 1972–1973, <https://doi.org/10.1093/bioinformatics/btp348>.
- [31] R. Lanfear, P.B. Frandsen, A.M. Wright, T. Senfeld, B. Calcott, Partitionfinder 2: new methods for selecting partitioned models of evolution for molecular and morphological phylogenetic analyses, Mol. Biol. Evol. 34 (3) (2017) 772–773, <https://doi.org/10.1093/molbev/msw260>.
- [32] L.T. Nguyen, H.A. Schmidt, A. von Haeseler, B.Q. Minh, Iq-tree: a fast and effective stochastic algorithm for estimating maximum-likelihood phylogenies, Mol. Biol. Evol. 32 (1) (2015) 268–274, <https://doi.org/10.1093/molbev/msu300>.
- [33] B.Q. Minh, M.A. Nguyen, A. von Haeseler, Ultrafast approximation for phylogenetic bootstrap, Mol. Biol. Evol. 30 (5) (2013) 1188–1195, <https://doi.org/10.1093/molbev/mst024>.
- [34] F. Ronquist, M. Teslenko, P. van der Mark, D.L. Ayres, A. Darling, S. Höhna, B. Larget, L. Liu, M.A. Suchard, J.P. Huelsenbeck, MrBayes 3.2: efficient bayesian phylogenetic inference and model choice across a large model space, Syst. Biol. 61 (3) (2012) 539–542, <https://doi.org/10.1093/sysbio/sys029>.
- [35] Y. Zhang, S. Feng, L. Fekrat, F. Jiang, M. Khathutshelo, Z. Li, The first two complete mitochondrial genome of *Dacus bivittatus* and *Dacus ciliatus* (Diptera: Tephritidae) by next-generation sequencing and implications for the higher phylogeny of tephritidae, Int. J. Biol. Macromol. 140 (2019) 469–476, <https://doi.org/10.1016/j.ijbiomac.2019.08.076>.
- [36] D.C.L. Teixeira, C. Powell, S. van Noort, C. Costa, M. Sinno, V. Caleca, C. Rhode, R.J. Kennedy, M. van Staden, B. van Asch, The complete mitochondrial genome of *Bactrocera biguttula* (Bezzi) (Diptera: tephritidae) and phylogenetic relationships with other Dacini, Int. J. Biol. Macromol. 126 (2019) 130–140, <https://doi.org/10.1016/j.ijbiomac.2018.12.186>.

- [37] Y. Zhang, S. Feng, Y. Zeng, H. Ning, L. Liu, Z. Zhao, F. Jiang, Z. Li, The first complete mitochondrial genome of *Bactrocera tsuneonis* (Miyake) (Diptera: Tephritidae) by next-generation sequencing and its phylogenetic implications, *Int. J. Biol. Macromol.* 118 (Pt A) (2018) 1229–1237, <https://doi.org/10.1016/j.ijbiomac.2018.06.099>.
- [38] J.P. Isaza, J.F. Alzate, N.A. Canal, Complete mitochondrial genome of the andean morphotype of *Anastrepha fraterculus* (Wiedemann) (Diptera: Tephritidae), *Mitochondrial Dna Part B-Resour* 2 (1) (2017) 210–211, <https://doi.org/10.1080/23802359.2017.1307706>.
- [39] S. Xu, Y. Wu, Y. Liu, P. Zhao, Z. Chen, F. Song, H. Li, W. Cai, Comparative mitogenomics and phylogenetic analyses of Pentatomoidea (Hemiptera: Heteroptera), *Genes* 12 (9) (2021), <https://doi.org/10.3390/genes12091306>.
- [40] J. Wang, Y. Wu, R. Dai, M. Yang, Comparative mitogenomes of six species in the subfamily lassinae (Hemiptera: Cicadellidae) and phylogenetic analysis, *Int. J. Biol. Macromol.* 149 (2020) 1294–1303, <https://doi.org/10.1016/j.ijbiomac.2020.01.270>.
- [41] L. Yan, W. Xu, D. Zhang, J. Li, Comparative analysis of the mitochondrial genomes of flesh flies and their evolutionary implication, *Int. J. Biol. Macromol.* 174 (2021) 385–391, <https://doi.org/10.1016/j.ijbiomac.2021.01.188>.
- [42] S.J. Wei, M. Shi, X.X. Chen, M.J. Sharkey, C. van Achterberg, G.Y. Ye, J.H. He, New views on strand asymmetry in insect mitochondrial genomes, *PLoS One* 5 (9) (2010) e12708, <https://doi.org/10.1371/journal.pone.0012708>.
- [43] O. Folmer, M. Black, W. Hoeh, R. Lutz, R. Vrijenhoek, DNA primers for amplification of mitochondrial cytochrome c oxidase subunit I from diverse metazoan invertebrates, *Mol. Mar. Biol. Biotechnol.* 3 (5) (1994) 294–299.
- [44] K.F. Armstrong, S.L. Ball, DNA barcodes for biosecurity: invasive species identification, *Philos. Trans. R. Soc. Lond. B Biol. Sci.* 360 (2005) 1813–1823, <https://doi.org/10.1098/rstb.2005.1713>.
- [45] P.D. Hebert, A. Cywinska, S.L. Ball, J.R. deWaard, Biological identifications through DNA barcodes, *Proc. Biol. Sci.* 270 (2003) 313, <https://doi.org/10.1098/rspb.2002.2218>.
- [46] H. Yang, T. Li, K. Dang, W. Bu, Compositional and mutational rate heterogeneity in mitochondrial genomes and its effect on the phylogenetic inferences of Cimicomorpha (Hemiptera: Heteroptera), *BMC Genom.* 19 (1) (2018) 264, <https://doi.org/10.1186/s12864-018-4650-9>.
- [47] D.N. Paul, T. Ryan Hebert, Gregory, the promise of DNA barcoding for taxonomy, *Syst. Biol.* (2005), <https://doi.org/10.1080/10635150500354886>.
- [48] M. Hu, N.B. Chilton, R.B. Gasser, The mitochondrial genomics of parasitic nematodes of socio-economic importance: recent progress, and implications for population genetics and systematics, *Adv. Parasitol.* 56 (2004) 133–212, [https://doi.org/10.1016/s0065-308x\(03\)56003-1](https://doi.org/10.1016/s0065-308x(03)56003-1).
- [49] P. Salvato, M. Simonato, A. Battisti, E. Negrisolo, The complete mitochondrial genome of the bag-shelter moth *Ochrogaster lunifer* (Lepidoptera, Notodontidae), *BMC Genom.* 9 (2008) 331, <https://doi.org/10.1186/1471-2164-9-331>.
- [50] H.X. Chen, S.C. Sun, P. Sundberg, W.C. Ren, J.L. Norenburg, A comparative study of nemertean complete mitochondrial genomes, including two new ones for *Nectonemertes cf. Mirabilis* and *Zygeupolia rubens*, may elucidate the fundamental pattern for the phylum Nemertea, *BMC Genom.* 13 (2012) 139, <https://doi.org/10.1186/1471-2164-13-139>.
- [51] D. Zhang, H. Zou, S.G. Wu, M. Li, I. Jakovli, J. Zhang, R. Chen, G.T. Wang, W.X. Li, Sequencing of the complete mitochondrial genome of a fish-parasitic flatworm *Paratetraonchoides inermis* (Platyhelminthes: Monogenea): trna gene arrangement reshuffling and implications for phylogeny, *Parasites Vectors* 10 (1) (2017) 462, <https://doi.org/10.1186/s13071-017-2404-1>.
- [52] Y. Hao, Y. Zou, Y. Ding, W. Xu, Z. Yan, X. Li, W. Fu, T. Li, B. Chen, Complete mitochondrial genomes of *Anopheles stephensi* and *An. dirus* and comparative evolutionary mitochonriomics of 50 mosquitoes, *Sci. Rep.* 7 (2017), <https://doi.org/10.1038/s41598-017-07977-0>.
- [53] H.J. Yang, Z.H. Yang, T.G. Ren, W.G. Dong, The complete mitochondrial genome of *Eulaelaps huzhuensis* (Mesostigmata:Haemogamasidae), *Exp. Appl. Acarol.* 90 (3–4) (2023) 301–316, <https://doi.org/10.1007/s10493-023-00802-6>.
- [54] D.H. Coucheron, M. Nymark, R. Breines, B.O. Karlsen, M. Andreassen, T.E. Jørgensen, T. Moum, S.D. Johansen, Characterization of mitochondrial mRNAs in codfish reveals unique features compared to mammals, *Curr. Genet.* 57 (3) (2011) 213–222, <https://doi.org/10.1007/s00294-011-0338-2>.
- [55] A.S. Reichert, M. Mori, Repair of tRNAs in metazoan mitochondria, *Nucleic Acids Res.* 28 (10) (2000) 2043–2048, <https://doi.org/10.1093/nar/28.10.2043>.
- [56] T.D. Do, D.W. Jung, C.B. Kim, Molecular phylogeny of selected *dorid nudibranchs* based on complete mitochondrial genome, *Sci. Rep.* 12 (1) (2022) 18797, <https://doi.org/10.1038/s41598-022-23400-9>.
- [57] X. Mengual, P. Kerr, A.L. Norrbom, N.B. Barr, M.L. Lewis, A.M. Stapelfeldt, S.J. Scheffer, P. Woods, M.S. Islam, C.A. Korytkowski, K. Uramoto, E.J. Rodriguez, B. D. Sutton, N. Nolzaco, G.J. Steck, S. Gaimari, Phylogenetic relationships of the *Tribe toxotrypanini* (Diptera: tephritidae) based on molecular characters, *Mol. Phylogenet. Evol.* 113 (2017) 84–112, <https://doi.org/10.1016/j.ympev.2017.05.011>.
- [58] M.L. Starkie, S.L. Cameron, M.N. Krosch, M.J. Phillips, J.E. Royer, M.K. Schutze, F. Strutt, A.D. Sweet, M.P. Zalucki, A.R. Clarke, A comprehensive phylogeny helps clarify the evolutionary history of host breadth and lure response in the australian dacini fruit flies (Diptera: Tephritidae), *Mol. Phylogenet. Evol.* 172 (2022) 107481, <https://doi.org/10.1016/j.ympev.2022.107481>.